

(repulsive) nonlinearity [7–25]. Very recently, the formation and stabilization of various localized gap modes [26–34] in nonlinear fractional systems (where the fractional diffraction is being a nonlocal integral operator [35–39]) with optical lattices are receiving growing interest.

On the other hand, moiré patterns, which connect the periodic (commensurate) structures and aperiodic (incommensurate) ones, as an artificially stacking twisted configuration of two periodic-lattice structures with a changeable rotation angle between them, have recently gained great research attention in many branches of physics thanks to its unique functionalities, including the so-called strongly correlated phenomena — Mott insulator states and unconventional superconductivity in magic-angle twisted bilayer graphene, flat band physics, etc. [40, 41]. A whole new field of research referred to as twistrionics has thus opened [42]. Moiré patterns provide unprecedented capabilities to the manipulation of electromagnetic/matter waves and enable precisely control of light–matter interactions with extraordinary optoelectronic properties that do not exist in single-layer superlattices (untwisted structures) [43]. Such twisted structures have pushed deep into the optics and photonics territory; particularly, photonic moiré lattices have firstly been imprinted in photorefractive crystals using optical induction method and light’s localization and delocalization [44] as well as geometry induced optical soliton formation therein [45] have been observed, stopped-light lasers in nanostructured moiré superlattice (optical magic-angle graphene) with remarkable figures of merit have been demonstrated [46]. Furthermore, self-trapping mechanisms in quadratic nonlinear media [47] and light bullets [48] as well as vortex solitons [49] with commensurate–incommensurate photonic moiré lattices were theoretically revealed, linear and nonlinear light localization at the edges of moiré lattices were observed [50], optical properties of bilayer graphene moiré superlattices in photonics were disclosed [51–54], and new understanding of electron-like properties in ultracold atoms trapped by twisted optical lattices was provided [55–57], other nonlinear effect (high harmonic generation) and flat band localization were addressed [58, 59]. Remarkably, a recent study proposed the creation of readily accessible moiré optical lattices in atomic ensembles by means of atomic coherence process called electromagnetically induced transparency [60]. Experimentally, the atomic Bose–Einstein condensates (BECs) have recently been made in twisted bilayer optical lattices and the corresponding quantum simulation as transition from superfluid to Mott insulator was observed [61]. Very recently, localized gap modes as gap solitons and vortices in aperiodic [62], periodic [63] and unique parity–time symmetric moiré optical lattices [64] were theoretically revealed and checked numerically.

In this work, we investigate, theoretically and numerically, the formation, structural, and stability properties of localized gap modes in nonlinear fractional systems

with two-dimensional (2D) shallow moiré optical lattices, which exhibit extremely flat bands, with particularly attention to the fundamental gap solitons and their architectural structures as bound states as well as topological states (gap vortices) with imprinted vortex charge $s = 1$ and 2. Highly localized feature of all the gap modes in the midst of underlying linear forbidden gaps are addressed, in an agreement with that of gap solitons in deep conventional optical lattices. With the usage of linear-stability analysis and direct perturbed simulations, we examine the (in-) stability properties of all the predicted localized gap modes in the norm as a function of chemical potential. Our findings suggest a new passage to study highly localized gap modes in nonlinear periodic systems with combined effects of linear nonlocality and shallow moiré patterns that exhibit extremely flat bands, and to compare them with those results reported in deep lattices.

2 The model

Our theory is in the framework of 2D nonlinear fractional Schrödinger equation (or Gross–Pitaevskii equation) for mean-field wave function ψ of particles (light waves as photons, ultracold atoms as BECs) moving by Lévy flights. According to our previous literature [34], the dimensionless model yields

$$i \frac{\partial \psi}{\partial t} = \frac{1}{2} (-\nabla^2)^{\alpha/2} \psi + V_{OL}(x, y)\psi + |\psi|^2 \psi, \quad (1)$$

where the fractional kinetic-energy operator is expressed by the direct and inverse Fourier-transform operators, \mathcal{F} and \mathcal{F}^{-1} , according to the fractional *Riesz derivative* [66]:

$$\begin{aligned} (-\nabla^2)^{\alpha/2} f(\mathbf{R}) &\equiv \mathcal{F}^{-1} [|\mathbf{K}|^\alpha \mathcal{F}(f)] \\ &= \frac{1}{(2\pi)^2} \int \int |\mathbf{K}|^\alpha \hat{f}(\mathbf{K}) \exp(i\mathbf{K} \cdot \mathbf{R}) d\mathbf{K}. \end{aligned} \quad (2)$$

Here α is the Lévy index (LI) with values $0 < \alpha \leq 2$, representing the diffraction order ($\alpha = 2$ being the conventional diffraction). Another form for the fractional diffraction term reads [67]

$$(-\Delta)^{\frac{\alpha}{2}} u(x) = C_{d,\alpha} P.V. \int_{\mathbb{R}^2} \frac{u(x) - u(x')}{|x - x'|^{d+\alpha}} dx', \quad (3)$$

where *P.V.* stands for the Cauchy principal value, and $|x - x'|$ denotes the Euclidean distance between points x and x' . The normalization constant $C_{d,\alpha}$ is defined as

$$C_{d,\alpha} = \frac{2^{\alpha-1} \alpha \Gamma((d + \alpha)/2)}{\sqrt{\pi^d} \Gamma(1 - \alpha/2)}, \quad (4)$$

with Γ being the Gamma function. It is relevant to stress that the fractional diffraction term (and thus the

fractional quantum mechanics) can be realized in quantum and condensed matter physics if the Lévy flights are substituted for the Brownian trajectories in Feynman path integrals [68–72]. In experiments, linear propagation of self-accelerating Airy pulses was realized in the optical Lévy waveguide with different values of LI α ($0 < \alpha \leq 2$) [39].

The 2D moiré optical lattice, $V_{OL}(x, y)$ in Eq. (1), under consideration yields

$$V_{OL}(x, y) = \epsilon_1(\cos^2 x + \cos^2 y) + \epsilon_2(\cos^2 x' + \cos^2 y'), \quad (5)$$

here $\epsilon_{1,2} > 0$ being depth (strength) of the two optical lattices with periodicity π . The strength contrast of the two sublattices is thus given by $p = \epsilon_2/\epsilon_1$, with $\epsilon_1 = 2$ throughout. A relative twisted angle θ associates the (x, y) plane with (x', y') plane, following

$$\begin{pmatrix} x' \\ y' \end{pmatrix} = \begin{pmatrix} \cos \theta & -\sin \theta \\ \sin \theta & \cos \theta \end{pmatrix} \begin{pmatrix} x \\ y \end{pmatrix}. \quad (6)$$

It can be seen that the moiré optical lattice Eq. (5) preserves the square lattice property as long as the Pythagorean angle $\theta = \arctan[2mn/(m^2 - n^2)]$ is satisfied, with the Pythagorean triples $(m^2 - n^2, 2mn, m^2 + n^2)$ at natural numbers (m, n) . Without loss of generality, below we restrict our discussion to the scenarios of $\theta = \arctan(3/4)$ and $\theta = \arctan(5/12)$ at natural numbers $(3, 1)$ and $(5, 1)$, respectively.

The stationary solution ϕ with chemical potential μ of Eq. (1) is solved as $\psi = \phi e^{-i\mu t}$, yielding

$$\mu\phi = \frac{1}{2}(-\nabla^2)^{\alpha/2}\phi + V_{OL}(x, y)\phi + |\phi|^2\phi. \quad (7)$$

For illustration, we define the norm (number of atoms in BECs or power in nonlinear optics) for such stationary solution as $N = \iint |\phi|^2 dx dy$.

The stability property is critical for a soliton, the usual evaluated way relies on linear-stability analysis. To this, we perturb the solution as $\psi = [\phi + \rho \exp(\lambda t) + \varrho^* \exp(\lambda^* t)] \exp(-i\mu t)$, where ϕ is the unperturbed solution obtained in Eq. (7), ρ and ϱ are small perturbations at eigenvalue λ . We substitute it into the Eq. (1) and get the linear eigenvalue equations:

$$\begin{pmatrix} L & \phi^2 \\ -\phi^{*2} & -L \end{pmatrix} \begin{pmatrix} \rho \\ \varrho \end{pmatrix} = i\lambda \begin{pmatrix} \rho \\ \varrho \end{pmatrix}, \quad (8)$$

where $L = -\mu + \frac{1}{2}(-\nabla^2)^{\alpha/2}\phi + 2|\phi|^2 + V_{OL}(x, y)$. The judgement follows the rule that the solutions are stable provided that all the real parts of the eigenvalues, obtained from Eq. (8), are nothing [$\text{Re}(\lambda) = 0$]; they are unstable otherwise.

Before presenting the numerical results, we introduce our numerical recipes here. First, we construct stationary localized solution from Eq. (7) by means of the modified squared-operator iteration method proposed in Ref. [65].

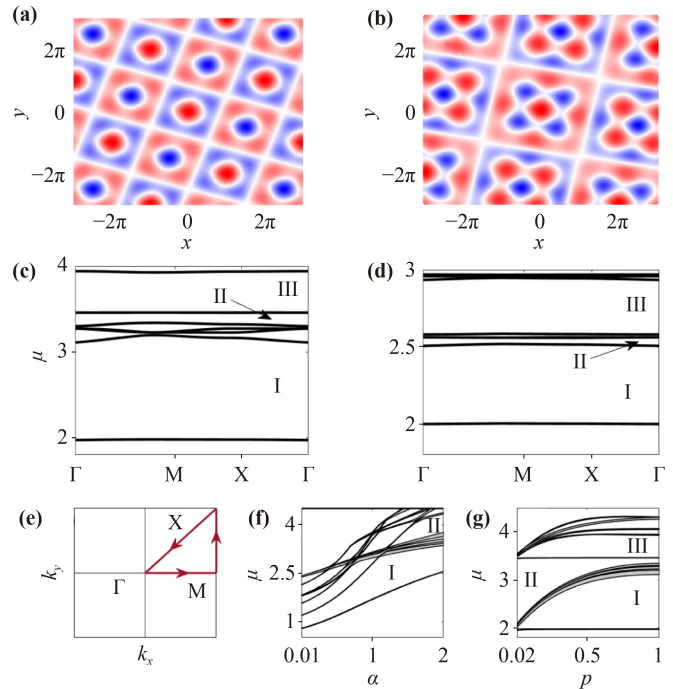


Fig. 1 Band-gap structures of 2D moiré square optical lattices at different twisted angles θ in fractional systems. Contour shapes of the moiré lattice (shaded blue, lattice potential minima; shaded red, lattice potential maxima) at $\theta = \arctan(3/4)$ (a) and $\theta = \arctan(5/12)$ (b) in real space, the corresponding band-gap structures, expressed as chemical potential μ vs. Bloch quasi-momentum \mathbf{k} in reciprocal lattice space, at $\alpha = 1.6$ are depicted in (c) and (d) respectively. (e) The first reduced Brillouin zone in the reciprocal lattice space; X, M, and Γ being the high-symmetry points. (f) Dependencies of μ on Lévy index α , and (g) on strength contrast p at $\alpha = 1.3$, and $\theta = \arctan(3/4)$. Regions I, II and III represent respectively the first, second, and third band gaps.

Second, its stability is measured by solving the linear-stability eigenvalue problem [Eq. (8)] via Fourier collocation method [65]. Lastly, the direct perturbed simulations of [Eq. (1)] via fourth-order Runge–Kutta method would tell us the stability reality.

3 Numerical results and discussion

3.1 Linear band-gap properties

The linear band-gap structure of the 2D moiré square optical lattices in Eq. (5) can be sought by solving the linearized Eq. (7) (discarding the last term). Figures 1(a) and (b) display the contour plots of such moiré lattices under the twisted angle $\theta = \arctan(3/4)$ and $\theta = \arctan(5/12)$ respectively, the corresponding band-gap structures are shown in Figs. 1(c) and (d) in the reciprocal lattice space given by Fig. 1(e). We are aware from Figs. 1(c) and (d) that the appearance of flat bands and wide first finite gap and the third one, while the second gap is

very narrow under a relatively lattice depth. With an increase of Lévy index α but at a given twisted angle [$\theta = \arctan(3/4)$], the band-gap structure becomes more complicated and more and more narrow gaps open, according to Fig. 1(f). Interestingly, when increasing strength contrast p of the two sublattices, both the first and third finite gaps widen, while the second gap narrows, as can be clearly seen from Fig. 1(g). These linear spectra demonstrate that the moiré optical lattices can be a breeding ground for the emergence of flat bands and band-gap engineering as well as the control of nonlinear wave localization (as will be shown below).

Before continuing, it is relevant to give the definition of localized gap modes (including but not limited to fundamental gap solitons and gap vortices) for readable and for public understanding. The localized gap modes are localized modes (could be excited as various forms) populated inside the finite gaps of the underlying linear Bloch spectrum of the nonlinear periodic physical models, they share some similarities of solitons and are existed because of an exquisite balance can be made between the linear diffraction/dispersion, periodic potentials and nonlinearity (of the system).

3.2 Fundamental gap solitons

As usual, we initially consider the first type of localized gap modes lying inside the finite gaps of the Pythagorean moiré optical lattices [Eq. (5)] under a twisted angle $\theta = \arctan(3/4)$. Such modes are fundamental gap solitons with isotropic profile, a characteristic example of which is provided in Fig. 2(a). By means of linear-stability analysis and the direct perturbed simulations, we find that they are stable when being excited in the midst of the given finite gaps while are unstable near the edges of flat bands, the latter case with more multiple side peaks is shown in Fig. 2(b). As pointed out elsewhere in previous publications [29, 30], the small Lévy index α can greatly influence the structure of the localized gap modes, which exhibits multiple modulated ripples, as figured out in Fig. 2(c). Systematic and detailed numerical calculations have helped us to build the relationship between the number of atoms (or norm N) and chemical potential μ at $p=0.3$ for fundamental gap solitons, according to Fig. 2(d). It is observed that the curve $N(\mu)$ matches the empirical stability criterion, the so-called “anti-Vakhitov–Kolokolov” (anti-VK) criterion, $dN/d\mu > 0$, a necessary but not a sufficient condition for deciding the stability of gap solitons in nonlinear physical systems with periodic potentials (photonic crystals/lattices and optical lattices) and repulsive nonlinearity [3, 14, 16–19, 73]. Note, particularly, that, in Fig. 2(d) the necessary N for generating a gap soliton can be small enough, contenting with the recent experimental observations of low power existence threshold for optical soliton formation controlled by angle twisting in photonic moiré optical lattices [52]. By simply increasing the LI α from

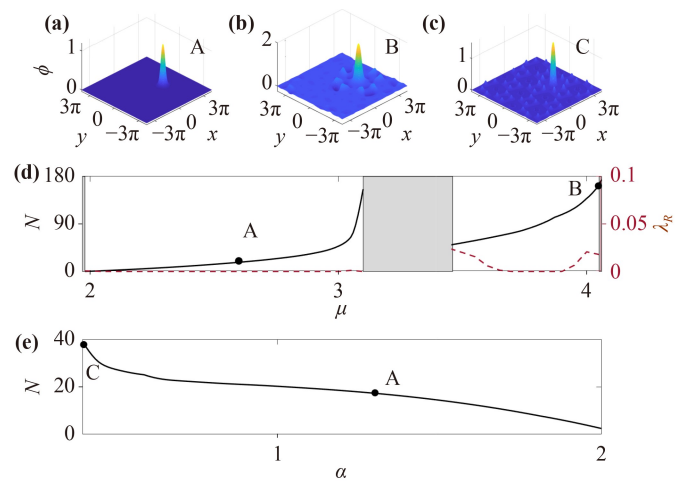


Fig. 2 Shapes of 2D fundamental gap solitons and the dependencies of norm N on chemical potential μ and Lévy index α in 2D moiré square optical lattices. (a–c) Characteristic shapes of fundamental gap solitons (GPs) at: (a) $\mu = 2.5$, $N = 17.4$ and $\alpha = 1.3$; (b) $\mu = 4.02$, $N = 144.1$ and $\alpha = 1.3$; (c) $\mu = 2.6$, $N = 38.98$ and $\alpha = 0.4$. (d) Norm N vs. chemical potential μ , and (e) vs. Lévy index (α). The linear-stability eigenvalues of gap solitons, expressed by the largest real part of the perturbation growth rate, $\lambda(R)$, are shown as red dashed line in (d). $\theta = \arctan(3/4)$ to all.

0 to 2, the gap soliton’s norm N fluctuates and then decreases, according to Fig. 2(e). Our direct perturbed evolutions in dynamical model [Eq. (1)] verify that the fundamental gap modes are exceptionally stable, with unstable ones only near the band edges.

3.3 Bound states composing of several gap solitons

We next investigate the formation and property of complex soliton structures that consist of several fundamental gap solitons; such modes can also be named as gap-soliton clusters. Typical profiles of the bound states of four- and three-soliton complexes are shown in Figs. 3(a), (b), and (c), displayed in the second line of Fig. 3 are their corresponding contour plots. It is seen that, owing to the structural twisting of the moiré lattices, these bound states are twisting localized gap modes with their centers deviate from coordinate origin (0,0). The bound states of several-soliton complexes and the vortex gap solitons carried with topological charge s reported below manifest the twisting property of localized multiple-soliton modes formed in the platform of moiré lattices. The $N(\mu)$ curve of these two classes of bound states is collected in Fig. 3(d), showing the increasing dependence within the finite gaps and a steeply increase close to the gap edges where exist stronger Bragg scattering and to compensate it a larger number of atoms is required accordingly. Once again, the bound states of several-gap-soliton complexes have wide stability regions within the midst of gaps, exemplified by our perturbed

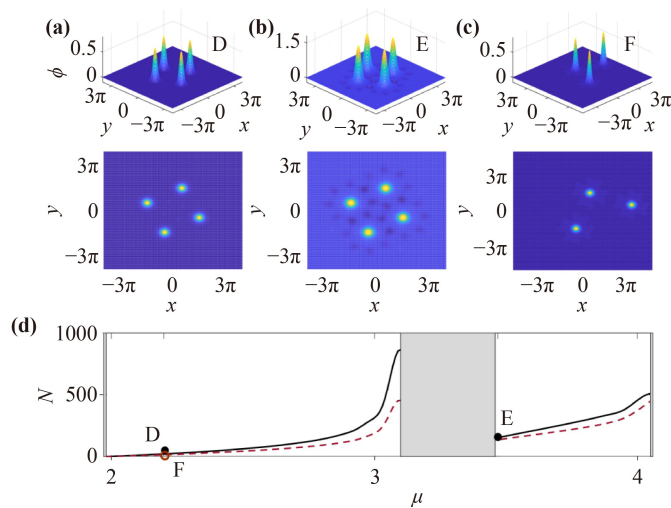


Fig. 3 Shapes and norm N vs. chemical potential μ of bound-state GSs in 2D moiré square optical lattices in nonlinear fractional system with Lévy index $\alpha = 1.3$. The 3D shapes (top), aerial views (central) and N vs. μ (bottom) of bound-state GSs. Parameters: (a) $\mu = 2.2$, $N = 20.85$; (b) $\mu = 3.47$, $N = 145.3$; (c) $\mu = 2.2$, $N = 14.72$. Marked points in (d) correspond to bound states shown in (a), (b), and (c); the first two are quadruple gap modes, the latter is triple mode of structure.

evolutions through directly solving dynamical model [Eq. (1)], as given below.

3.4 Vortex gap solitons with topological charge $s = 1, 2$

The bound states of several gap solitons reported above are localized modes without phase connecting, when introducing phase to combine all the bright peaks, the vortex gap solitons (or gap vortices) are generated. To launch vortex solutions, it is relevant to associate the rotational symmetry of the physical system with the topological charge of states, as pointed out in previous literature [74]. The simplest type of vortex gap solitons is the one with quadruple structures, which are rhombic sets of four fundamental gap solitons, zero in the center, and spaced by $\pi/2$ phase shifts between each, forming the 2π entire phase circulation (topological charge $s = 1$). Characteristic profiles of such vortex gap solitons are displayed in Figs. 4(a) and (b). For the case of topological charge $s = 2$, the phase circulation is 4π , and the associated vortex gap solitons could be built as sets of eight bright peaks, as sampled in Figs. 4(c) and (d). In the second and third lines of the figure, we have shown the corresponding contour plots of profiles and phase distributions

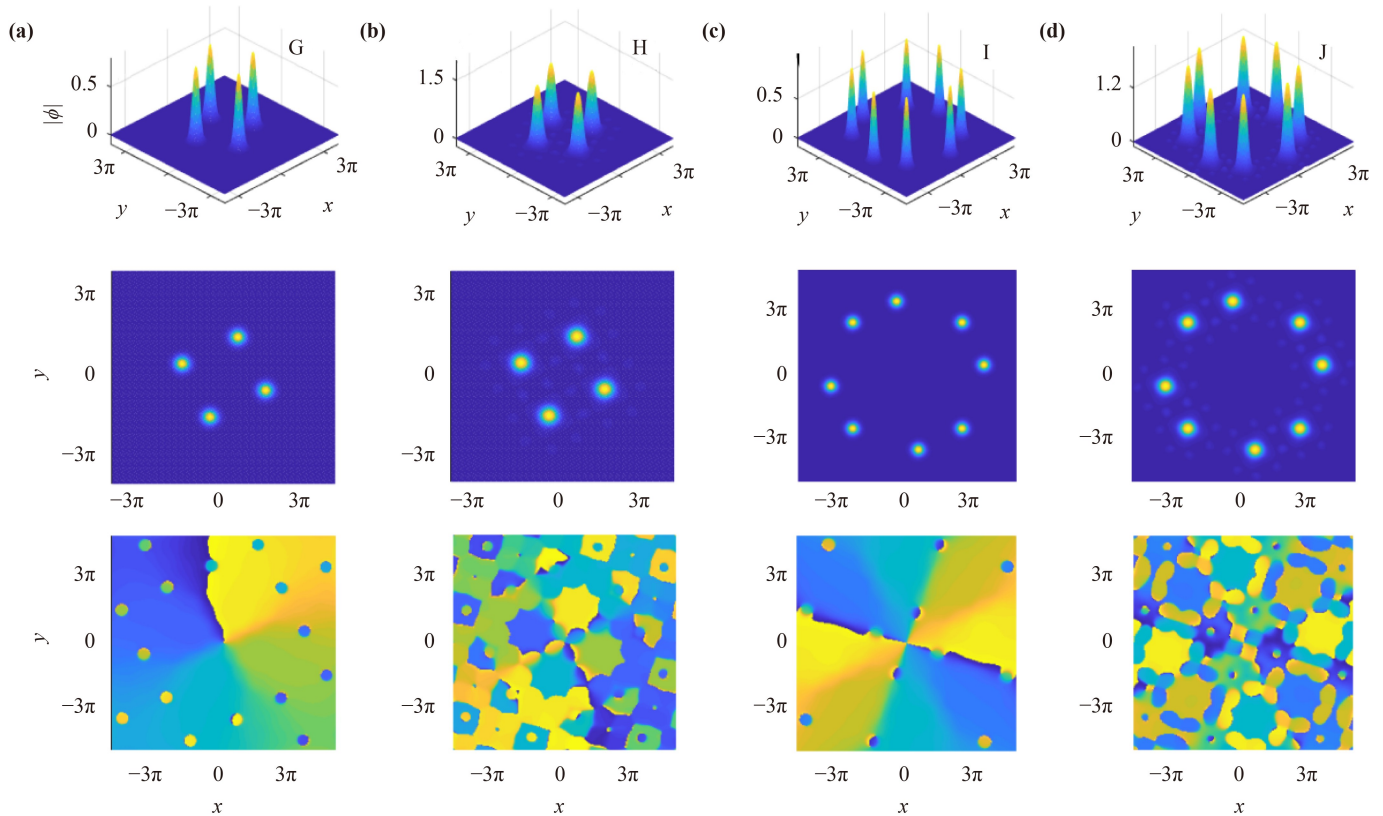


Fig. 4 Shapes and topological phases of vortex gap solitons with imprinted vorticity s in 2D moiré square optical lattices in nonlinear fractional system with Lévy index $\alpha = 1.3$. The 3D shapes (top), aerial views (second line), phase structures (third line). Parameters: (a) $\mu = 2.3$, $N = 31.67$; (b) $\mu = 3.5$, $N = 306.52$; (c) $\mu = 2.4$, $N = 133.78$; (d) $\mu = 3.85$, $N = 1306$. Vorticity $s = 1$ for (a, b) and $s = 2$ for (c, d). The vortex solutions in (a, b, c, d) correspond respectively to the marked points (G, H, I, J) from Fig. 5(a).

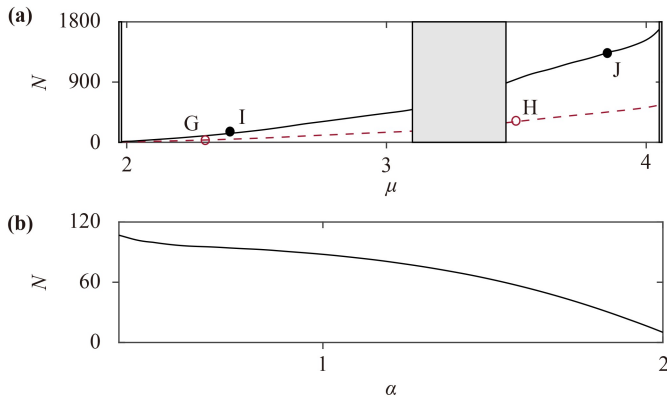


Fig. 5 Norm N vs. chemical potential μ (a) ($\alpha = 1.3$) and Lévy index α (b) ($\mu = 2.6$) of vortex gap solitons with imprinted vorticity s . Other parameters: (a) vorticity (topological charge) $s = 1$ for black line and $s = 2$ for red dashed line; (b) $s = 1$.

of these vortex gap solitons imprinted with $s = 2$. The $N(\mu)$ dependences of these vortex gap solitons with topological charge $s = 1$ and $s = 2$ are summed in Fig. 5(a), which follows once again the anti-VK criterion, $dN/d\mu > 0$ [3, 14, 16, 17, 18, 19, 73]. And the $N(\alpha)$ dependence of these vortex gap solitons with topological charge $s = 1$ are summed in Fig. 5(b).

Stability and instability properties of these vortices are confirmed in direct perturbed simulations of dynamic equation [Eq. (1)], stressing that they are very

stable in finite gaps and are unstable close to the edge of gaps.

3.5 Perturbed dynamics of fundamental gap solitons and bound states

To illustrate the general rule of direct perturbed dynamics of the localized gap modes thus found in moiré optical lattices, Figs. 6(a) and (b) depict, respectively, profiles of the stable and unstable fundamental gap solitons populated within the first finite gap and near the band edge, and the associated perturbed dynamics and N vs. time are shown in the second line. It is observed that the unstable gap solitons are close to the band edge and side peaks increase during the unstable evolutions, while the stable one can keep their norm (number of atoms) almost constant and is accompanied by a weak number fluctuation.

As far as the bound states, which consist of the arrangement of several fundamental gap solitons, are concerned, their profiles, stability and instability dynamics of four-soliton complexes are displayed in Figs. 6(c) and (d) and the following second and third lines, showing that they resemble very much with their fundamental ones in the process of perturbed evolutions. We emphasize that the evolutionary cases of vortex gap solitons are resembled the same stable and unstable dynamical processes, according to stable and unstable examples of vortex gap solitons with vorticity $s = 1$ in Figs. 6(e) and (f).

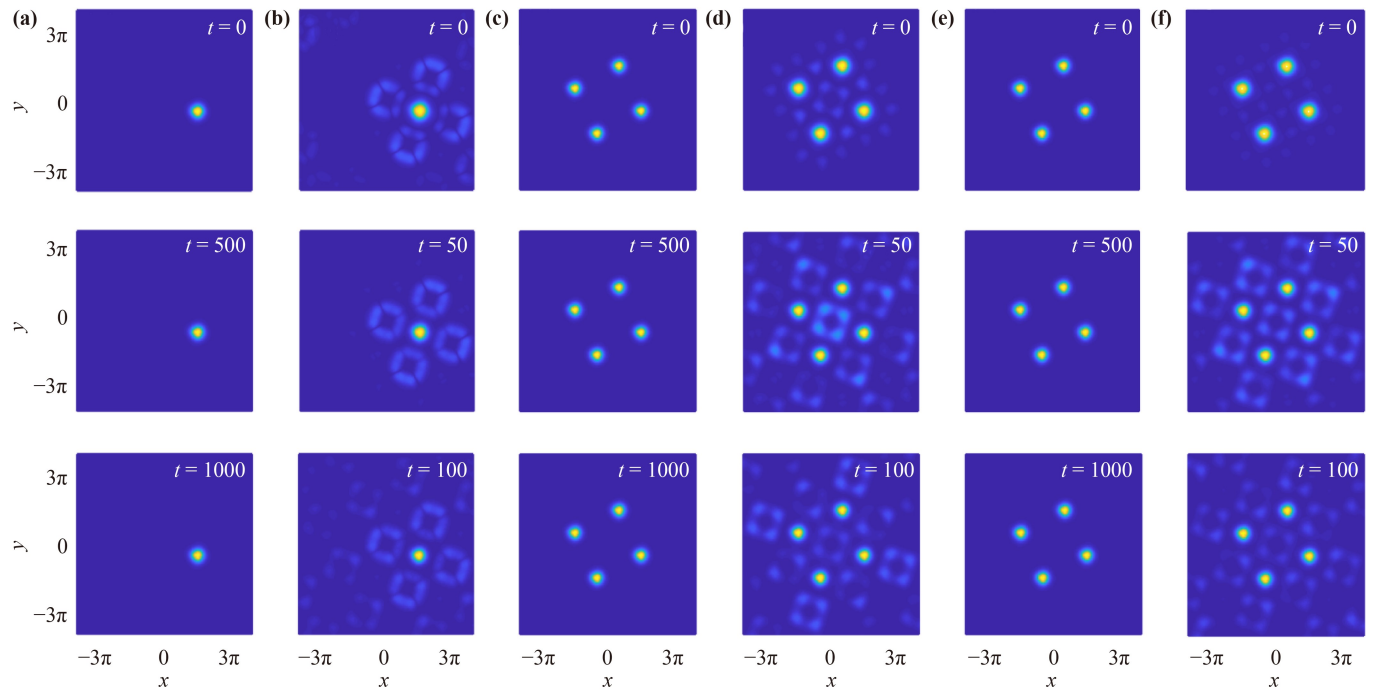


Fig. 6 Dynamics of fundamental GSs (a, b), higher-order GSs (c, d), and gap vortices with vorticity $s = 1$ (e, f) supported by the 2D moiré square optical lattices. Other parameters: (a) $\mu = 2.5, N = 13.61$; (b) $\mu = 4.02, N = 140.9$; (c) $\mu = 2.2, N = 20.85$; (d) $\mu = 3.47, N = 145.3$; (e) $\mu = 2.3, N = 31.67$; (f) $\mu = 3.5, N = 306.52$.

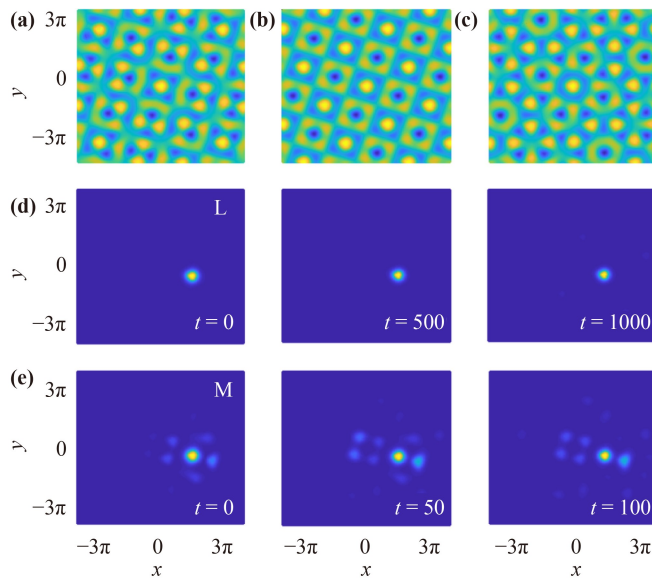


Fig. 7 Contour shapes of the moiré lattice (shaded blue, lattice potential minima; shaded yellow, lattice potential maxima) at $\theta = \arctan(3/4) - 0.1$ (a), $\theta = \arctan(3/4)$ (b) and $\theta = \arctan(3/4) + 0.1$ (c). Perturbed evolution in real time of stable (d) and unstable (e) fundamental gap solitons supported by non-periodic moiré optical lattices under the non-Pythagorean angle $\theta = \arctan(3/4) - 0.1$. Other parameters: (d) $\mu = 2.4, N = 5.59$; (e) $\mu = 3.05, N = 39.34$. $\alpha = 1.3$ for all.

3.6 Localized gap modes supported by moiré optical lattices under non-Pythagorean angle

It is also an interesting issue to address the formation and dynamics of localized gap modes in the physical framework of nonlinear fractional media with 2D moiré optical lattices but under the condition of non-Pythagorean angle. As pointed out in previous publication [43], the width of finite gaps of the underlying linear spectrum shrinks greatly by tuning to the non-Pythagorean angles, it is therefore a good choice to just launch a localized gap mode for the moiré square optical lattices with twist angle just slightly deviates from the Pythagorean one. The contour shapes of the moiré lattice with different twisted angles are displayed in Figs. 7(a), (b) and (c), corresponding respectively to $\theta = \arctan(3/4) - 0.1$ (a), $\theta = \arctan(3/4)$ (b) and $\theta = \arctan(3/4) + 0.1$ (c), showing the losing of spatial translation periodicity for the former and the last, both of which deviate from a perfect periodic one [the middle, Fig. 7(b)]. As an example, in Figs. 7(d) and (e), we display the formation of stable and unstable fundamental gap solitons supported by non-periodic moiré optical lattices with twist angle $\theta = \arctan(3/4) - 0.1$, the corresponding time evolutions of both gap solitons are very similar to those presented in Fig. 6, demonstrating that the stable one keeps its coherence, while the unstable one diverges.

4 Conclusion

In summary, we have addressed, numerically and theoretically, the nonlinear localization of Bose–Einstein condensates (BECs) or nonlinear light wave propagation in nonlinear fractional media with 2D moiré square optical lattices, investigating the structural properties and dynamics of various localized gap modes like fundamental gap solitons, bound states of three- and four-soliton complexes, gap vortices with vortex charge $s = 1$ and 2. The latter two classes of gap modes are twisting modes since the twisting structural property of moiré lattices. All these localized gap modes are stable inside the finite gaps and are unstable approach the flat Bloch bands, basing on our linear-stability analysis and systematic direct perturbed evolutions. The results predicted here could expand our understanding of soliton physics in nonlinear periodic physical systems having two linear tunable degrees of freedom: linear nonlocality (fractional-order diffraction) and twisted shallow moiré patterns that exhibit extremely flat bands and could be useful in the comparison with the similarities and differences of those reported in literature with very deep but untwisted conventional lattices.

Declarations The authors declare that they have no competing interests and there are no conflicts.

Acknowledgements This work was supported by the National Natural Science Foundation of China (NSFC) (No. 12074423), Young Scholar of Chinese Academy of Sciences in Western China (No. XAB2021YN18), and China Postdoctoral Science Foundation (No. 2023M733722).

References

1. Y. S. Kivshar and G. P. Agrawal, *Optical Solitons: From Fibers to Photonic Crystals*, Academic, San Diego, 2003
2. O. Morsch and M. Oberthaler, Dynamics of Bose–Einstein condensates in optical lattices, *Rev. Mod. Phys.* 78(1), 179 (2006)
3. Y. V. Kartashov, B. A. Malomed, and L. Torner, Solitons in nonlinear lattices, *Rev. Mod. Phys.* 83(1), 247 (2011)
4. I. L. Garanovich, S. Longhi, A. A. Sukhorukov, and Y. S. Kivshar, Light propagation and localization in modulated photonic lattices and waveguides, *Phys. Rep.* 518(1–2), 1 (2012)
5. V. V. Konotop, J. Yang, and D. A. Zezyulin, Nonlinear waves in *PT*-symmetric systems, *Rev. Mod. Phys.* 88(3), 035002 (2016)
6. Y. V. Kartashov, G. E. Astrakharchik, B. A. Malomed, and L. Torner, Frontiers in multidimensional self-trapping of nonlinear fields and matter, *Nat. Rev. Phys.* 1(3), 185 (2019)
7. B. J. Eggleton, R. E. Slusher, C. M. de Sterke, P. A. Krug, and J. E. Sipe, Bragg grating solitons, *Phys. Rev.*

- Lett.* 76(10), 1627 (1996)
8. D. Mandelik, R. Morandotti, J. S. Aitchison, and Y. Silberberg, Gap solitons in waveguide arrays, *Phys. Rev. Lett.* 92(9), 093904 (2004)
 9. O. Peleg, G. Bartal, B. Freedman, O. Manela, M. Segev, and D. N. Christodoulides, Conical diffraction and gap solitons in honeycomb photonic lattices, *Phys. Rev. Lett.* 98(10), 103901 (2007)
 10. B. Eiermann, T. Anker, M. Albiez, M. Taglieber, P. Treutlein, K. P. Marzlin, and M. K. Oberthaler, Bright Bose–Einstein gap solitons of atoms with repulsive interaction, *Phys. Rev. Lett.* 92(23), 230401 (2004)
 11. Th. Anker, M. Albiez, R. Gati, S. Hunsmann, B. Eiermann, A. Trombettoni, and M. K. Oberthaler, Nonlinear self-trapping of matter waves in periodic potentials, *Phys. Rev. Lett.* 94(2), 020403 (2005)
 12. F. H. Bennet, T. J. Alexander, F. Haslinger, A. Mitchell, D. N. Neshev, and Y. S. Kivshar, Observation of nonlinear self-trapping of broad beams in defocusing waveguide arrays, *Phys. Rev. Lett.* 106(9), 093901 (2011)
 13. C. Bersch, G. Onishchukov, and U. Peschel, Optical gap solitons and truncated nonlinear Bloch waves in temporal lattices, *Phys. Rev. Lett.* 109(9), 093903 (2012)
 14. L. Zeng and J. Zeng, Gap-type dark localized modes in a Bose–Einstein condensate with optical lattices, *Adv. Photonics* 1(4), 046004 (2019)
 15. J. Shi and J. Zeng, Self-trapped spatially localized states in combined linear-nonlinear periodic potentials, *Front. Phys.* 15(1), 12602 (2020)
 16. J. Li and J. Zeng, Dark matter-wave gap solitons in dense ultra-cold atoms trapped by a one-dimensional optical lattice, *Phys. Rev. A* 103(1), 013320 (2021)
 17. J. Chen and J. Zeng, Dark matter-wave gap solitons of Bose–Einstein condensates trapped in optical lattices with competing cubic–quintic nonlinearities, *Chaos Solitons Fractals* 150, 111149 (2021)
 18. Z. Chen and J. Zeng, Localized gap modes of coherently trapped atoms in an optical lattice, *Opt. Express* 29(3), 3011 (2021)
 19. Z. Chen and J. Zeng, Two-dimensional optical gap solitons and vortices in a coherent atomic ensemble loaded on optical lattices, *Commun. Nonlinear Sci. Numer. Simul.* 102, 105911 (2021)
 20. Z. Chen and J. Zeng, Nonlinear localized modes in one-dimensional nanoscale dark-state optical lattices, *Nanophotonics* 11(15), 3465 (2022)
 21. J. Li, Y. Zhang, and J. Zeng, Matter-wave gap solitons and vortices in three-dimensional parity–time-symmetric optical lattices, *iScience* 25(4), 104026 (2022)
 22. J. Li, Y. Zhang, and J. Zeng, 3D nonlinear localized gap modes in Bose–Einstein condensates trapped by optical lattices and space-periodic nonlinear potentials, *Adv. Photon. Res.* 3(7), 2100288 (2022)
 23. J. Qin and L. Zhou, Supersolid gap soliton in a Bose–Einstein condensate and optical ring cavity coupling system, *Phys. Rev. E* 105(5), 054214 (2022)
 24. J. Yang and Y. Zhang, Spin–orbit-coupled spinor gap solitons in Bose–Einstein condensates, *Phys. Rev. A* 107(2), 023316 (2023)
 25. Z. Chen, Z. Wu, and J. Zeng, Light gap bullets in defocusing media with optical lattices, *Chaos Solitons Fractals* 174, 113785 (2023)
 26. C. Huang and L. Dong, Gap solitons in the nonlinear fractional Schrödinger equation with an optical lattice, *Opt. Lett.* 41(24), 5636 (2016)
 27. C. Huang, C. Li, H. Deng, and L. Dong, Gap Solitons in fractional dimensions with a quasi-periodic lattice, *Ann. Phys.* 531(9), 1900056 (2019)
 28. J. Xie, X. Zhu, and Y. He, Vector solitons in nonlinear fractional Schrödinger equations with parity–time-symmetric optical lattices, *Nonlinear Dyn.* 97(2), 1287 (2019)
 29. L. Zeng and J. Zeng, One-dimensional gap solitons in quintic and cubic–quintic fractional nonlinear Schrödinger equations with a periodically modulated linear potential, *Nonlinear Dyn.* 98, 985 (2019)
 30. L. Zeng and J. Zeng, Preventing critical collapse of higher-order solitons by tailoring unconventional optical diffraction and non-linearities, *Commun. Phys.* 3(1), 26 (2020)
 31. X. Zhu, F. Yang, S. Cao, J. Xie, and Y. He, Multipole gap solitons in fractional Schrödinger equation with parity–time-symmetric optical lattices, *Opt. Express* 28(2), 1631 (2020)
 32. L. Zeng, M. R. Belić, D. Mihalache, J. Shi, J. Li, S. Li, X. Lu, Y. Cai, and J. Li, Families of gap solitons and their complexes in media with saturable nonlinearity and fractional diffraction, *Nonlinear Dyn.* 108(2), 1671 (2022)
 33. Y. Y. Bao, S. R. Li, Y. H. Liu, and T. F. Xu, Gap solitons and non-linear Bloch waves in fractional quantum coupler with periodic potential, *Chaos Solitons Fractals* 156, 111853 (2022)
 34. X. Liu, B. A. Malomed, and J. Zeng, Localized modes in nonlinear fractional systems with deep lattices, *Adv. Theory Simul.* 5(4), 2100482 (2022)
 35. L. Dong and C. Huang, Double-hump solitons in fractional dimensions with a PT -symmetric potential, *Opt. Express* 26(8), 10509 (2018)
 36. C. Huang and L. Dong, Beam propagation management in a fractional Schrödinger equation, *Sci. Rep.* 7(1), 5442 (2017)
 37. N. Laskin, *Fractional Quantum Mechanics*, World Scientific, 2018
 38. B. A. Malomed, Optical solitons and vortices in fractional media: A mini-review of recent results, *Photonics* 8(9), 353 (2021)
 39. S. Liu, Y. Zhang, B. A. Malomed, and E. Karimi, Experimental realizations of the fractional Schrödinger equation in the temporal domain, *Nat. Commun.* 14(1), 222 (2023)
 40. Y. Cao, V. Fatemi, S. Fang, K. Watanabe, T. Taniguchi, E. Kaxiras, and P. Jarillo-Herrero, Unconventional superconductivity in magic-angle graphene superlattices, *Nature* 556(7699), 43 (2018)
 41. Y. Cao, V. Fatemi, A. Demir, S. Fang, S. L. Tomarken, J. Y. Luo, J. D. Sanchez-Yamagishi, K. Watanabe, T. Taniguchi, E. Kaxiras, R. C. Ashoori, and P. Jarillo-Herrero, Correlated insulator behaviour at half-filling in magic-angle graphene superlattices, *Nature* 556(7699), 80 (2018)



42. S. Carr, D. Massatt, S. Fang, P. Cazeaux, M. Luskun, and E. Kaxiras, Twistronics: Manipulating the electronic properties of two-dimensional layered structures through their twist angle, *Phys. Rev. B* 95(7), 075420 (2017)
43. C. Huang, F. Ye, X. Chen, Y. V. Kartashov, V. V. Konotop, and L. Torner, Localization–delocalization wavepacket transition in Pythagorean aperiodic potentials, *Sci. Rep.* 6(1), 32546 (2016)
44. P. Wang, Y. Zheng, X. Chen, C. Huang, Y. V. Kartashov, L. Torner, V. V. Konotop, and F. Ye, Localization and delocalization of light in photonic moiré lattices, *Nature* 577(7788), 42 (2020)
45. Q. Fu, P. Wang, C. Huang, Y. V. Kartashov, L. Torner, V. V. Konotop, and F. Ye, Optical soliton formation controlled by angle twisting in photonic moiré lattices, *Nat. Photonics* 14(11), 663 (2020)
46. X. R. Mao, Z. K. Shao, H. Y. Luan, S. L. Wang, and R. M. Ma, Magic-angle lasers in nanostructured moiré superlattice, *Nat. Nanotechnol.* 16(10), 1099 (2021)
47. Y. V. Kartashov, F. Ye, V. V. Konotop, and L. Torner, Multi-frequency solitons in commensurate-incommensurate photonic moiré lattices, *Phys. Rev. Lett.* 127(16), 163902 (2021)
48. Y. V. Kartashov, Light bullets in moiré lattices, *Opt. Lett.* 47(17), 4528 (2022)
49. S. K. Ivanov, V. V. Konotop, Y. V. Kartashov, and L. Torner, Vortex solitons in moiré optical lattices, *Opt. Lett.* 48(14), 3797 (2023)
50. A. A. Arkhipova, Y. V. Kartashov, S. K. Ivanov, S. A. Zhuravitskii, N. N. Skryabin, I. V. Dyakonov, A. A. Kalinkin, S. P. Kulik, V. O. Kompanets, S. V. Chekalin, F. Ye, V. V. Konotop, L. Torner, and V. N. Zadkov, Observation of linear and nonlinear light localization at the edges of moiré arrays, *Phys. Rev. Lett.* 130(8), 083801 (2023)
51. S. S. Sunku, G. X. Ni, B. Y. Jiang, H. Yoo, A. Sternbach, A. S. McLeod, T. Stauber, L. Xiong, T. Taniguchi, K. Watanabe, P. Kim, M. M. Fogler, and D. N. Basov, Photonic crystals for nano-light in moiré graphene superlattices, *Science* 362(6419), 1153 (2018)
52. W. J. M. Kort-Kamp, F. J. Culchac, R. B. Capaz, and F. A. Pinheiro, Photonic spin Hall effect in bilayer graphene moiré superlattices, *Phys. Rev. B* 98(19), 195431 (2018)
53. G. Hu, Q. Ou, G. Si, Y. Wu, J. Wu, Z. Dai, A. Krasnok, Y. Mazor, Q. Zhang, Q. Bao, C. W. Qiu, and A. Alù, Topological polaritons and photonic magic angles in twisted α -MoO₃ bilayers, *Nature* 582(7811), 209 (2020)
54. M. Chen, X. Lin, T. H. Dinh, Z. Zheng, J. Shen, Q. Ma, H. Chen, P. Jarillo-Herrero, and S. Dai, Configurable phonon polaritons in twisted α -MoO₃, *Nat. Mater.* 19(12), 1307 (2020)
55. A. González-Tudela and J. I. Cirac, Cold atoms in twisted-bilayer optical potentials, *Phys. Rev. A* 100(5), 053604 (2019)
56. T. Salamon, A. Celi, R. W. Chhajlany, I. Frérot, M. Lewenstein, L. Tarruell, and D. Rakshit, Simulating twistronics without a twist, *Phys. Rev. Lett.* 125(3), 030504 (2020)
57. X. W. Luo and C. Zhang, Spin-twisted optical lattices: Tunable flat bands and Larkin–Ovchinnikov superfluids, *Phys. Rev. Lett.* 126(10), 103201 (2021)
58. T. Ning, Y. Ren, Y. Huo, and Y. Cai, Efficient high harmonic generation in nonlinear photonic moiré superlattice, *Front. Phys.* 18(5), 52305 (2023)
59. Z. Ma, W. J. Chen, Y. Chen, J. H. Gao, and X. C. Xie, Flat band localization due to self-localized orbital, *Front. Phys.* 18(6), 63302 (2023)
60. Z. Chen, X. Liu, and J. Zeng, Electromagnetically induced moiré optical lattices in a coherent atomic gas, *Front. Phys.* 17(4), 42508 (2022)
61. Z. Meng, L. Wang, W. Han, F. Liu, K. Wen, C. Gao, P. Wang, C. Chin, and J. Zhang, Atomic Bose–Einstein condensate in twisted-bilayer optical lattices, *Nature* 615(7951), 231 (2023)
62. C. Huang, L. Dong, H. Deng, X. Zhang, and P. Gao, Fundamental and vortex gap solitons in quasiperiodic photonic lattices, *Opt. Lett.* 46(22), 5691 (2021)
63. X. Liu and J. Zeng, Matter-wave gap solitons and vortices of dense Bose–Einstein condensates in moiré optical lattices, *Chaos Solitons Fractals* 174, 113869 (2023)
64. X. Liu and J. Zeng, Gap solitons in parity–time symmetric moiré optical lattices, *Photon. Res.* 11(2), 196 (2023)
65. J. Yang, *Nonlinear Waves in Integrable and Nonintegrable Systems*, SIAM: Philadelphia, 2010
66. M. Cai and C. P. Li, On Riesz derivative, *Fract. Calc. Appl. Anal.* 22(2), 287 (2019)
67. S. Duo and Y. Zhang, Accurate numerical methods for two and three dimensional integral fractional Laplacian with applications, *Comput. Methods Appl. Mech. Eng.* 355, 639 (2019)
68. N. Laskin, Fractional quantum mechanics and Lévy path integrals, *Phys. Lett. A* 268(4–6), 298 (2000)
69. N. Laskin, Fractional quantum mechanics, *Phys. Rev. E* (3), 3135 (2000)
70. N. Laskin, Fractional Schrödinger equation, *Phys. Rev. E* 66(5), 056108 (2002)
71. L. Zhang, C. Li, H. Zhong, C. Xu, D. Lei, Y. Li, and D. Fan, Propagation dynamics of super-Gaussian beams in fractional Schrödinger equation: From linear to nonlinear regimes, *Opt. Express* 24(13), 14406 (2016)
72. L. Zhang, Z. He, C. Conti, Z. Wang, Y. Hu, D. Lei, Y. Li, and D. Fan, Modulational instability in fractional nonlinear Schrödinger equation, *Commun. Nonlinear Sci. Numer. Simul.* 48, 531 (2017)
73. M. Vakhitov and A. Kolokolov, Stationary solutions of the wave equation in a medium with nonlinearity saturation, *Radiophys. Quantum Electron.* 16(7), 783 (1973)
74. A. Ferrando, M. Zacarés, and M. A. García-March, Vorticity cutoff in nonlinear photonic crystals, *Phys. Rev. Lett.* 95(4), 043901 (2005)